

# Coronal parameters in Seyfert galaxies: the NuSTAR view and the future IXPE perspectives



AGN13

BEAUTY  
and the  
BEAST

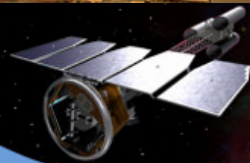
Alessia Tortosa

AGN 13 - 10/10/2018 - Milan

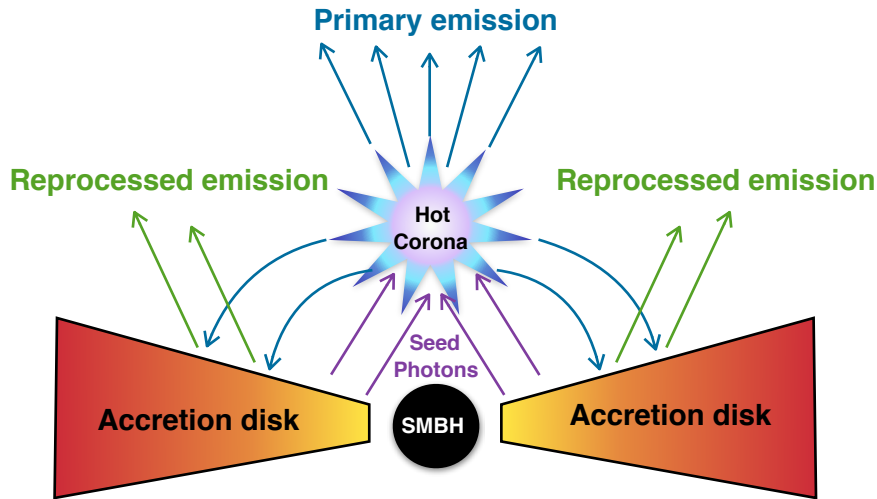


**IXPE**

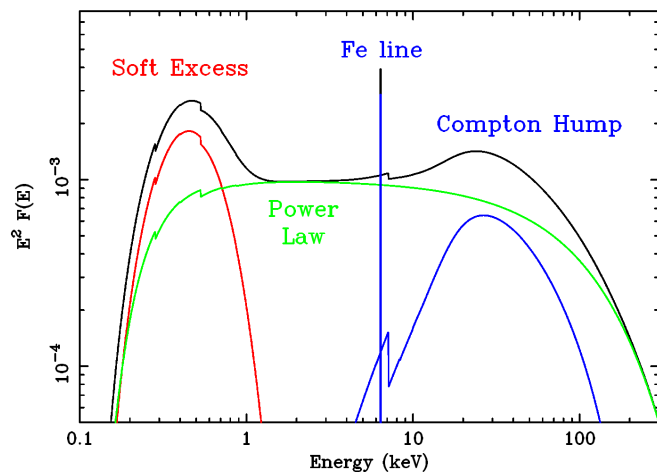
Imaging X-Ray Polarimetry Explorer



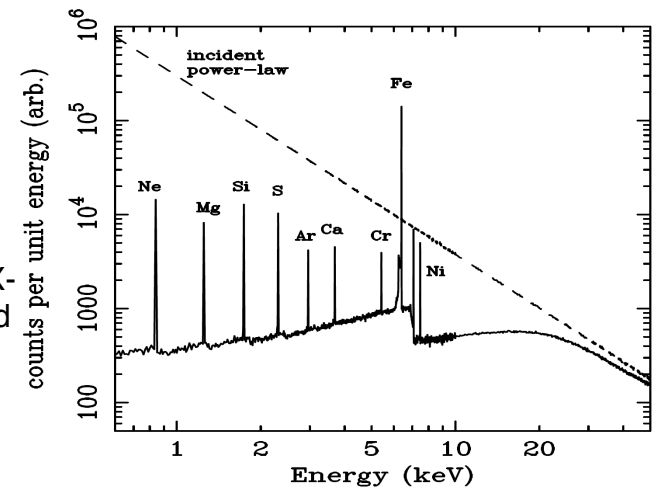
## Two Phase Model:



- Hot, optically thin, X-ray emitting **corona**;
- Cold, optically thick, UV-optical emitting **accretion disc**.



- **Primary Power-law:** with photon index and cutoff energy directly related to the temperature and to the optical depth of the coronal plasma. Comptonization models imply  $E_c = 2-3 \times kT_e$ .
- **Reprocessed Emission:** Typical X-ray features of the reflection by cold circumnuclear material include intense Fe  $K\alpha$  line at 6.4 keV and the associated Compton reflection continuum peaking at  $\sim 30$  keV.

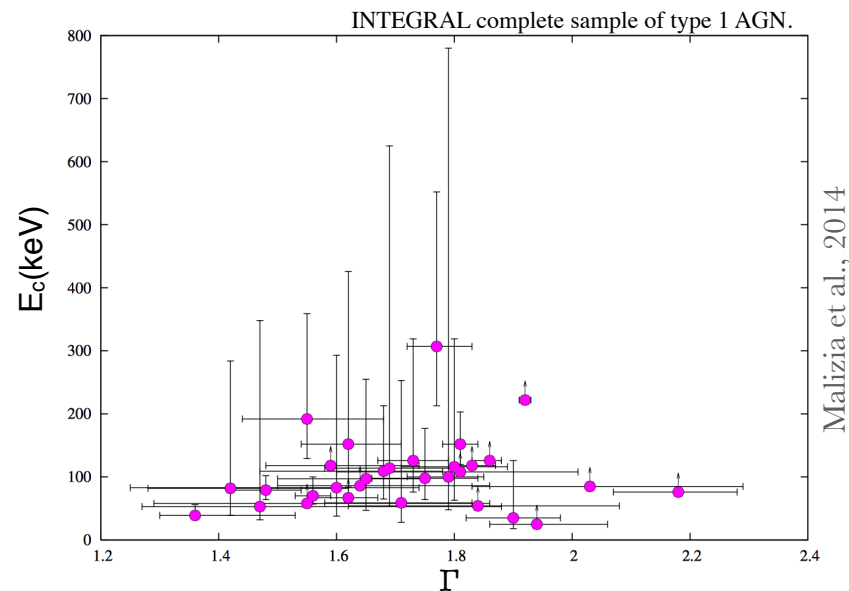
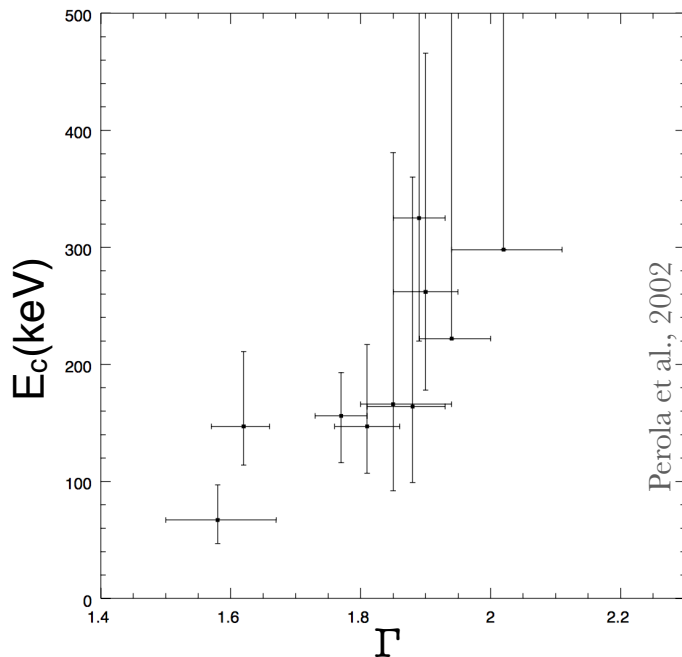


# CUTOFF MEASUREMENTS

Analysis of a sample to have insights into the average properties of AGN.

- Non-Focusing and therefore background-dominated instruments (BeppoSAX, INTEGRAL, Swift);
- Degeneracies between parameters;
- Uncertainties;
- High energy cutoff values correlated with the photon index of the primary emission.

Photon index - cutoff correlation in the BeppoSAX sample



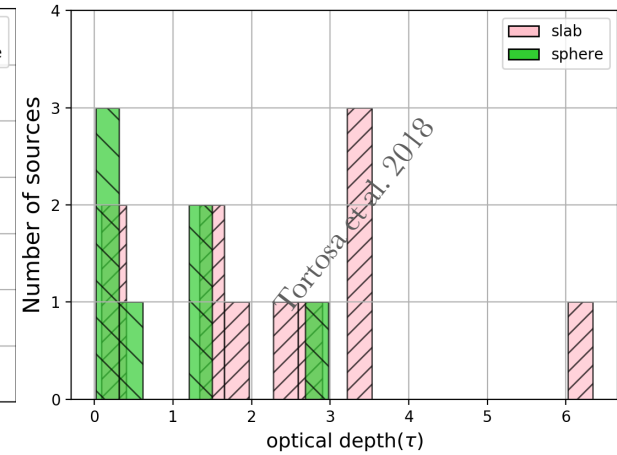
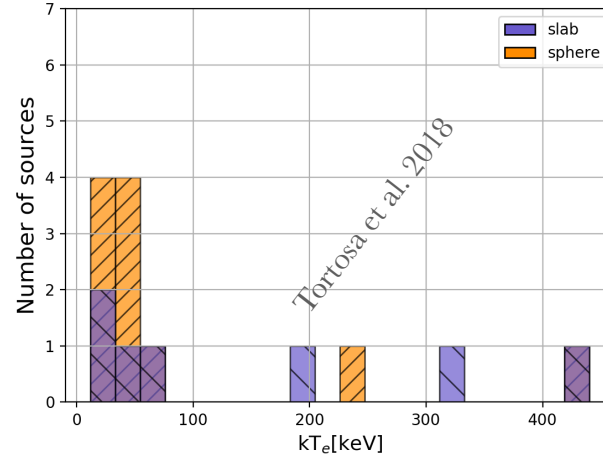
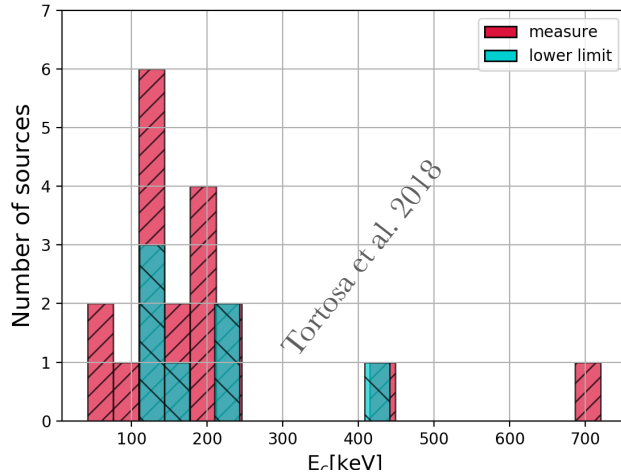
New observations of *NuSTAR*, *XMM-Newton* and *Swift* X-ray satellites & archival data.

## 19 Bright Nearby Seyfert Galaxies:

- Unobscured ( $N_{\text{H}} \leq 6 \times 10^{22} \text{ cm}^{-2}$ ), to have a clear view of the primary emission component;
- Present in the *Swift*-BAT 70-month catalogue;
- Observed by *NuSTAR* and other X-rays observatories;
- *Objects for which the cut-off energy had been left fixed in the spectral analysis are not included (e.g. 1H0707-495)*

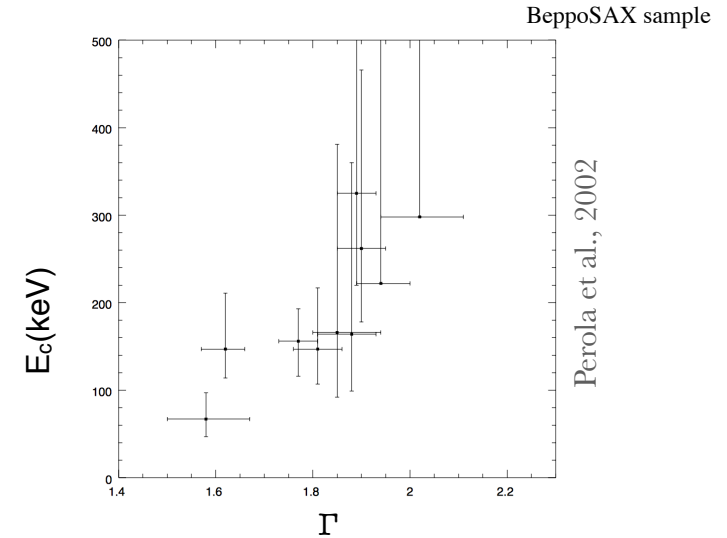
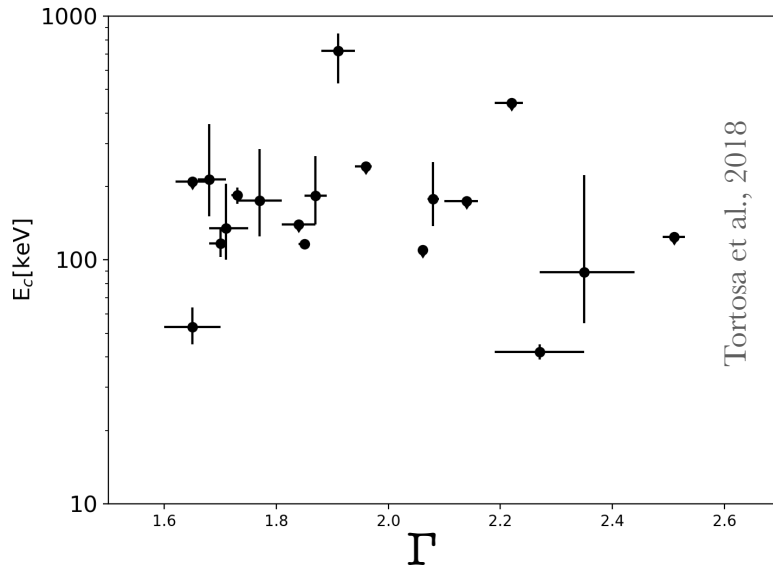
Source	Ref.	$\Gamma$	$E_c$ [keV]	$\log(M_{\text{bh}}/M_{\odot})$	Ref.	$L_{\text{bol}}/L_{\text{Edd}}$	$L_{2-10\text{keV}}$ ergs s <sup>-1</sup>	$F_{2-10\text{keV}}$ erg cm <sup>-2</sup> s <sup>-1</sup>	$kT_e$ [keV]	$\tau$	geom.	model
NGC 5506	1	$1.91 \pm 0.03$	$720^{+130}_{-190}$	$8.0 \pm 0.2$	(A)	0.006	0.053	6.2	$440^{+230}_{-250}$	$0.02^{+0.2}_{-0.01}$	slab	COMP TT
									$440^{+230}_{-250}$	$0.09^{+0.2}_{-0.01}$	sphere	COMP TT
MCG -05-23-16	2	$1.85 \pm 0.01$	$170 \pm 5$	$7.7 \pm 0.2$	(B)	0.058	0.18	10.4	$30 \pm 2$	$1.2 \pm 0.1$	slab	COMP TT
									$25 \pm 2$	$3.5 \pm 0.02$	sphere	COMP TT
SWIFT J2127.4	3-4	$2.08 \pm 0.01$	$180^{+75}_{-40}$	$7.2 \pm 0.2$	(J)	0.136	0.14	2.9	$70^{+40}_{-30}$	$0.5^{+0.3}_{-0.2}$	slab	COMP TT
									$50^{+30}_{-25}$	$1.4^{+1.0}_{-0.7}$	sphere	COMP TT
IC4329A	5-6	$1.73 \pm 0.01$	$185 \pm 15$	$8.08 \pm 0.3$	(N)	0.125	0.56	12.0	$37 \pm 7$	$1.3 \pm 0.1$	slab	COMP TT
									$33 \pm 6$	$3.4 \pm 0.5$	sphere	COMP TT
3C390.3	7	$1.70 \pm 0.01$	$120 \pm 20$	$8.4 \pm 0.4$	(H)	0.241	1.81	4.03	$40 \pm 20$	$3.3^{+1.3}_{-2.8}$	sphere	COMP TT
3C382	8	$1.68 \pm 0.03$	$215^{+150}_{-60}$	$9.2 \pm 0.5$	(D)	0.072	2.34	2.9	$330 \pm 30$	$0.2 \pm 0.02$	slab	COMP TT
GRS 1734-292	9	$1.65 \pm 0.05$	$53 \pm 10$	$8.5 \pm 0.1$	(L)	0.036	0.056	2.9	$12 \pm 1$	$2.9 \pm 0.2$	slab	COMP TT
									$12^{+1.7}_{-1.2}$	$6.3 \pm 0.3$	sphere	COMP TT
NGC 6814	10	$1.71 \pm 0.04$	$135^{+70}_{-35}$	$7.0 \pm 0.1$	(C)	0.003	0.021	0.2	$45^{+100}_{-20}$	$2.5^{\dagger} \pm 0.5$	sphere	NTHCOMP
MCG +8-11-11	10	$1.77 \pm 0.04$	$175^{+110}_{-50}$	$7.2 \pm 0.2$	(E)	0.754	0.51	5.6	$60^{+110}_{-30}$	$1.9^{\dagger} \pm 0.4$	sphere	NTHCOMP
Ark 564	11	$2.27 \pm 0.08$	$42 \pm 3$	$6.8 \pm 0.5$	(H)	1.313	0.39	-	$15 \pm 2$	$2.7^{\dagger} \pm 0.2$	sphere	NTHCOMP
PG 1247+267	12-13	$2.35 \pm 0.09$	$90^{+130}_{-35}$	$8.9 \pm 0.2$	(M)	0.11	0.79	0.05	$46^{+60}_{-20}$	$1.4^{\dagger} \pm 0.3$	sphere	NTHCOMP
Ark 120	14-15	$1.87 \pm 0.02$	$180^{+80}_{-40}$	$8.2 \pm 0.1$	(H)	0.085	0.92	2.3	-	-	-	-
NGC 7213	16	$1.84 \pm 0.03$	$> 140$	$8.0 \pm 0.2$	(G)	0.001	0.012	1.3	$230^{+70}_{-250}$	$0.2 \pm 0.1$	sphere	COMP PS
MCG 6-30-15	17-18	$2.06 \pm 0.01$	$> 110$	$6.4 \pm 0.1$	(E)	0.238	0.056	5.5	-	-	-	-
NGC 2110	19	$1.65 \pm 0.03$	$> 210$	$8.3 \pm 0.2$	(K)	0.016	0.35	12.5	$190 \pm 130$	$0.2 \pm 0.1$	slab	COMP TT
Mrk 335	21-22	$2.14 \pm 0.03$	$> 174$	$7.2 \pm 0.1$	(H)	0.284	0.18	1.9	-	-	-	-
Fairall 9	20	$1.95 \pm 0.02$	$> 242$	$8.1 \pm 0.7$	(H)	0.054	0.60	2.9	-	-	-	-
Mrk 766	17-23-24	$2.22 \pm 0.03$	$> 441$	$6.3 \pm 0.1$	(I)	1.254	0.046	1.4	-	-	-	-
PG 1211+143	26	$2.51 \pm 0.2$	$> 124$	$8.2 \pm 0.2$	(H)	0.047	0.35	1.0	-	-	-	-

## Distribution of some of the investigated parameters:



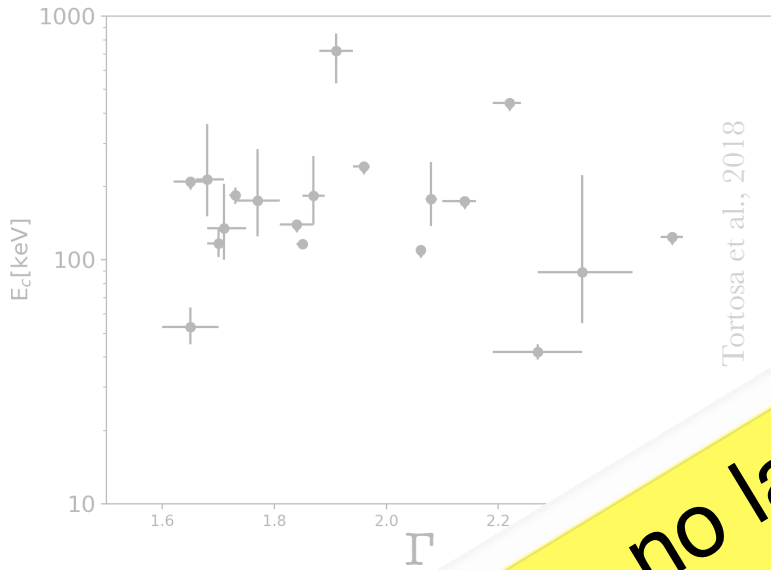
- ◆ Search for correlations between spectral and physical parameters to have an overview of the physics and the structure of the hot corona

X	Y	$\rho$	$h_0$	geometry
$\Gamma$	$E_c$	0.18	0.47	-
$\log(M_{bh}/M_\odot)$	$E_c$	-0.11	0.61	-
$L_{bol}/L_{Edd}$	$E_c$	-0.14	0.56	-
$\tau$	$kT_e$	-0.88	0.004	slab
$\tau$	$kT_e$	-0.63	0.02	sphere
$\log(M_{bh}/M_\odot)$	$\tau$	-0.22	0.63	slab
$\log(M_{bh}/M_\odot)$	$\tau$	-0.26	0.46	sphere
$L_{bol}/L_{Edd}$	$\tau$	0.49	0.27	slab
$L_{bol}/L_{Edd}$	$\tau$	0.38	0.28	sphere
$\log(M_{bh}/M_\odot)$	$kT_e$	0.20	0.64	slab
$\log(M_{bh}/M_\odot)$	$kT_e$	0.18	0.47	sphere
$L_{bol}/L_{Edd}$	$kT_e$	-0.37	0.41	slab
$L_{bol}/L_{Edd}$	$kT_e$	-0.36	0.32	sphere



- ◆ Search for correlations between spectral and physical parameters to have an overview of the physics and the structure of the hot corona
- ◆ The only correlation found is between the optical depth and the coronal temperature in both spherical and slab geometry of the corona.

X	Y	$\rho$	$h_0$	geometry
$\Gamma$	$E_c$	0.18	0.47	-
$\log(M_{bh}/M_\odot)$	$E_c$	-0.11	0.61	-
$L_{bol}/L_{Edd}$	$E_c$	-0.14	0.56	-
$\tau$	$kT_e$	-0.88	0.004	slab
$\tau$	$kT_e$	-0.63	0.02	sphere
$\log(M_{bh}/M_\odot)$	$\tau$	-0.22	0.63	slab
$\log(M_{bh}/M_\odot)$	$\tau$	-0.26	0.46	sphere
$L_{bol}/L_{Edd}$	$\tau$	0.49	0.27	slab
$L_{bol}/L_{Edd}$	$\tau$	0.38	0.28	sphere
$\log(M_{bh}/M_\odot)$	$kT_e$	0.20	0.64	slab
$\log(M_{bh}/M_\odot)$	$kT_e$	0.18	0.47	sphere
$L_{bol}/L_{Edd}$	$kT_e$	-0.37	0.41	slab
$L_{bol}/L_{Edd}$	$kT_e$	-0.36	0.32	sphere



Tortosa et al., 2018



Perola et al., 2002

**There are no large systematics in the NuSTAR measurements!!!**

- ◆ Search for correlations between spectral and structural parameters. We have analyzed the structure of the emission line region.
- ◆ The only correlation found is between the optical depth and the coronal temperature. This is consistent with spherical and slab geometry of the emission line region.

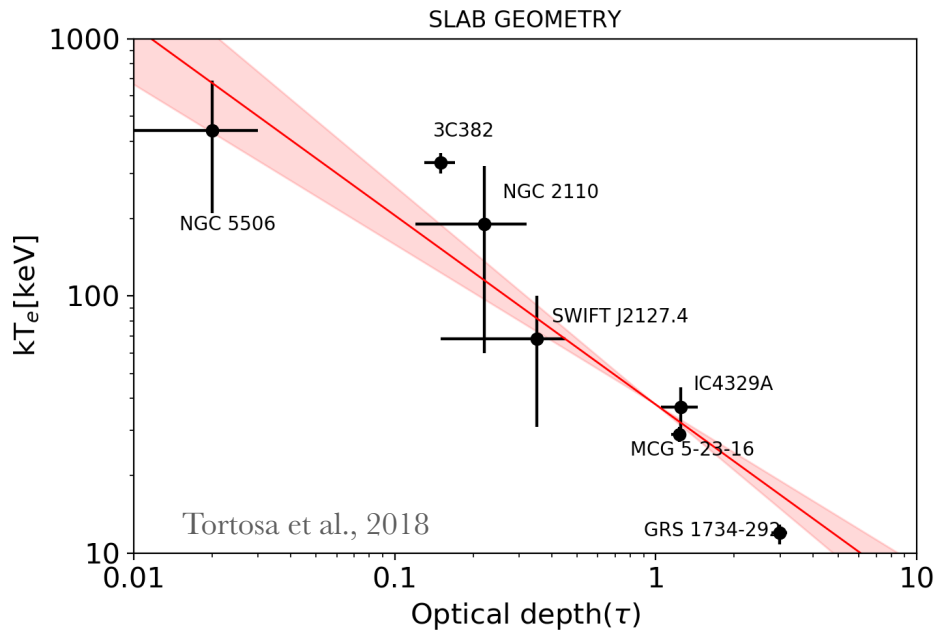
	Y	$\rho$	$h_0$	geometry
$\Gamma$	$E_c$	0.18	0.47	-
$\log(M_{bh}/M_\odot)$	$E_c$	-0.11	0.61	-
$L_{bol}/L_{Edd}$	$E_c$	-0.14	0.56	-
$\tau$	$kT_e$	-0.88	0.004	slab
$\tau$	$kT_e$	-0.63	0.02	sphere
$\log(M_{bh}/M_\odot)$	$\tau$	-0.22	0.63	slab
$\log(M_{bh}/M_\odot)$	$\tau$	-0.26	0.46	sphere
$L_{bol}/L_{Edd}$	$\tau$	0.49	0.27	slab
$L_{bol}/L_{Edd}$	$\tau$	0.38	0.28	sphere
$\log(M_{bh}/M_\odot)$	$kT_e$	0.20	0.64	slab
$\log(M_{bh}/M_\odot)$	$kT_e$	0.18	0.47	sphere
$L_{bol}/L_{Edd}$	$kT_e$	-0.37	0.41	slab
$L_{bol}/L_{Edd}$	$kT_e$	-0.36	0.32	sphere

# CORONAL PARAMETERS

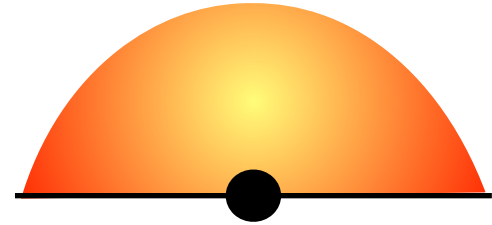
## Slab geometry



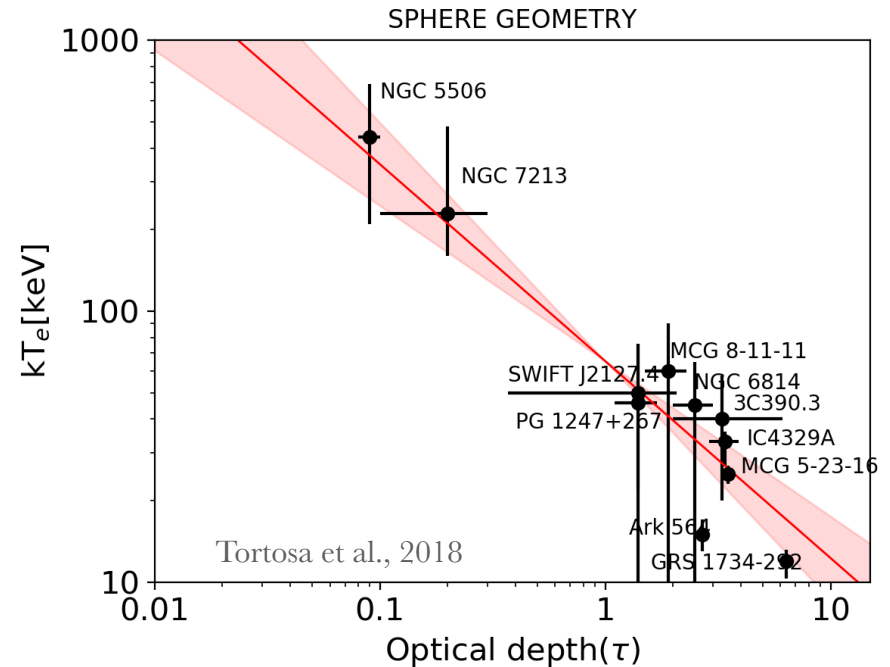
$$\text{Log}(kT_e) = (-0.7 \pm 0.1)\text{Log}(\tau) + (1.6 \pm 0.06)$$



## Spherical geometry



$$\text{Log}(kT_e) = (-0.7 \pm 0.2)\text{Log}(\tau) + (1.8 \pm 0.1)$$



# CORONAL PARAMETERS

The parameters are model-dependent BUT they are obtained with different models!

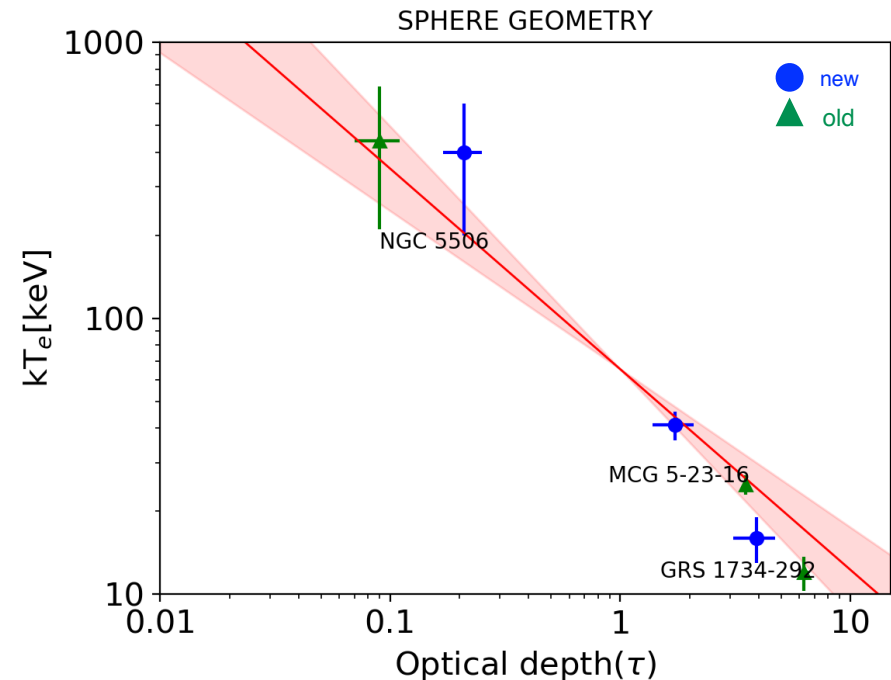
Double check on NGC 5506, GRS 1734-292 and MCG -05-23-16 which have the most extreme values of  $\tau$  and  $kT_e$

## New Values (NTHCOMP)

Source	$\Gamma$	$kT_e$ (keV)	$\tau$
NGC 5506	$1.73^{+0.09}_{-0.03}$	$400 \pm 200$	0.21
GRS 1734-292	$1.81 \pm 0.04$	$16 \pm 3$	3.9
MCG -05-23-16	$1.93 \pm 0.01$	$41 \pm 5$	1.73

## Old Values (COMPTT)

Source	$\Gamma$	$kT_e$ (keV)	$\tau$
NGC 5506	$1.91 \pm 0.03$	$440^{+230}_{-250}$	0.09
GRS 1734-292	$1.65 \pm 0.05$	$12 \pm 1$	6.3
MCG -05-23-16	$1.85 \pm 0.01$	$25 \pm 2$	1.2



# CORONAL PARAMETERS

Fixed disc-corona configuration in radiative balance

**Fixed** heating/cooling ratio

~~correlation~~

The coronal geometry is the same for all Seyfert galaxies

+

The corona is in radiative balance

=

We would expect  $\tau$  and/or  $kT_e$  to cluster around the same values for all the objects of our sample.

Why are  $\tau$  and  $kT_e$  strongly anti-correlated?

# CORONAL PARAMETERS

Fixed disc-corona configuration in radiative balance

**Fixed** heating/cooling ratio

~~correlation~~

The coronal geometry is the same for all Seyfert galaxies

+

~~The corona is in radiative balance~~

=

We would expect  $\tau$  and/or  $kT_e$  to cluster around the same values for all the objects of our sample.

Variation of the intrinsic disk emission.

↑ disc intrinsic emission , ↑ corona cooling, ↓ temperature.

NGC 5506 : ↓ disc intrinsic emission

GRS 1734-292 : ↑ disc intrinsic emission

# CORONAL PARAMETERS

Fixed disc-corona configuration in radiative balance

**Fixed** heating/cooling ratio

~~correlation~~

~~The coronal geometry is the same for all Seyfert galaxies~~

+

The corona is in radiative balance

=

We would expect  $\tau$  and/or  $kT_e$  to cluster around the same values for all the objects of our sample.

## Geometrical variation of the Corona

$R_{tr}$  and/or  $H \downarrow$ ,  $\uparrow$  corona cooling,  $\downarrow$  temperature.

NGC 5506 :  $\uparrow R_{tr}$  and/or  $H$

GRS 1734-292:  $\downarrow R_{tr}$  and/or  $H$

**ASTROPHYSICS WITH IXPE  
(IMAGING X-RAY  
POLARIMETRY EXPLORER)**



**ALESSIA TORTOSA**

# IMAGING X-RAY POLARIMETRY EXPLORER

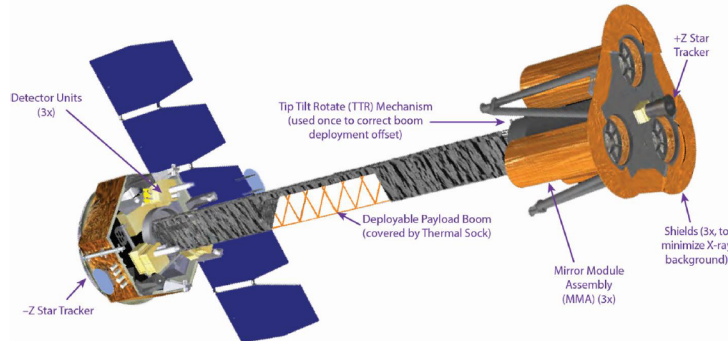
NASA SMEX Missions in development; it will fly in April 2021

- 40 years from the last positive measurement;
- 2 order of magnitude more sensitive over the X-ray polarimeter aboard the Orbiting Solar Observatory OSO8;
- Dramatic improvement in sensitivity: from one to hundred sources!

X-ray polarimetry will open a new observational window, adding the two missing observables in X-rays: **polarization degree & angle.**

## Scientific topics:

- Acceleration phenomena
- Pulsar wind nebulae
- SNR
- Jets
- Emission in strong magnetic fields
- Pulsars, Magnetars
- AGN & XRB
- QED effects
- GR effects close to accreting BHs
- Quantum gravity



**IXPE is going to observe almost all classes of X-ray sources.**

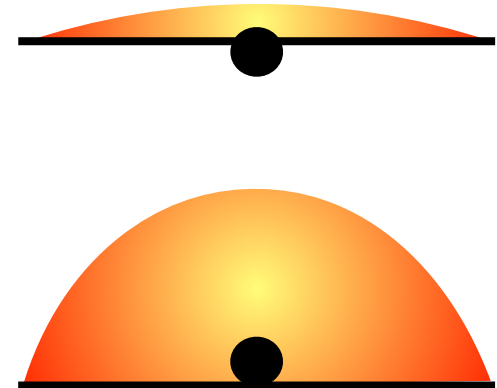
# HOT CORONAE AND POLARIZATION

The Comptonization process imprints weak, energy dependent, polarization features on the emerging spectra.

These polarization features depend on the relative geometry of the incident photons and scattering electrons.

The geometry is related to the corona origin:

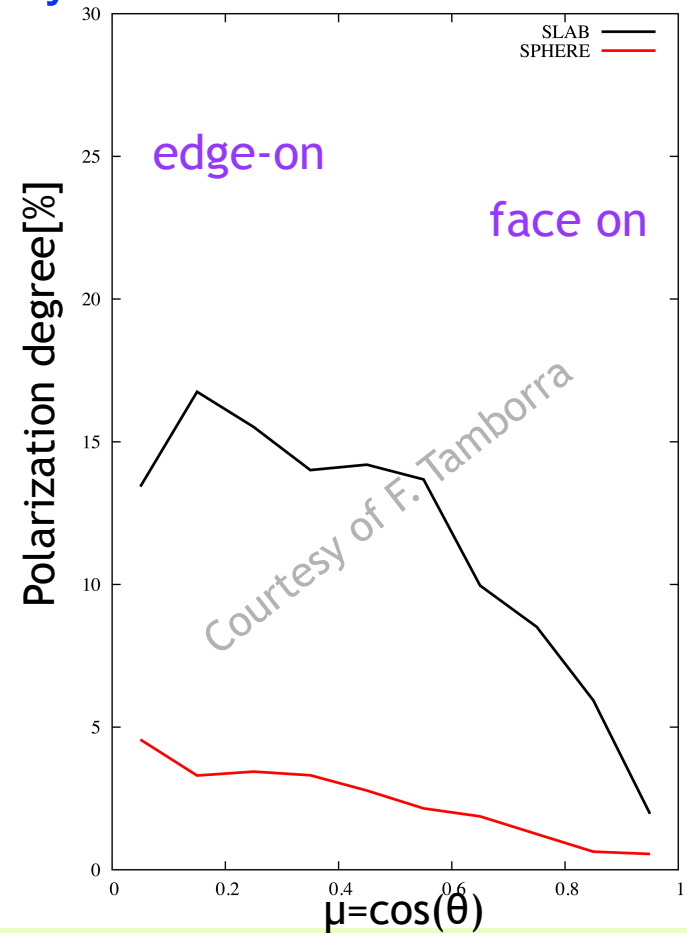
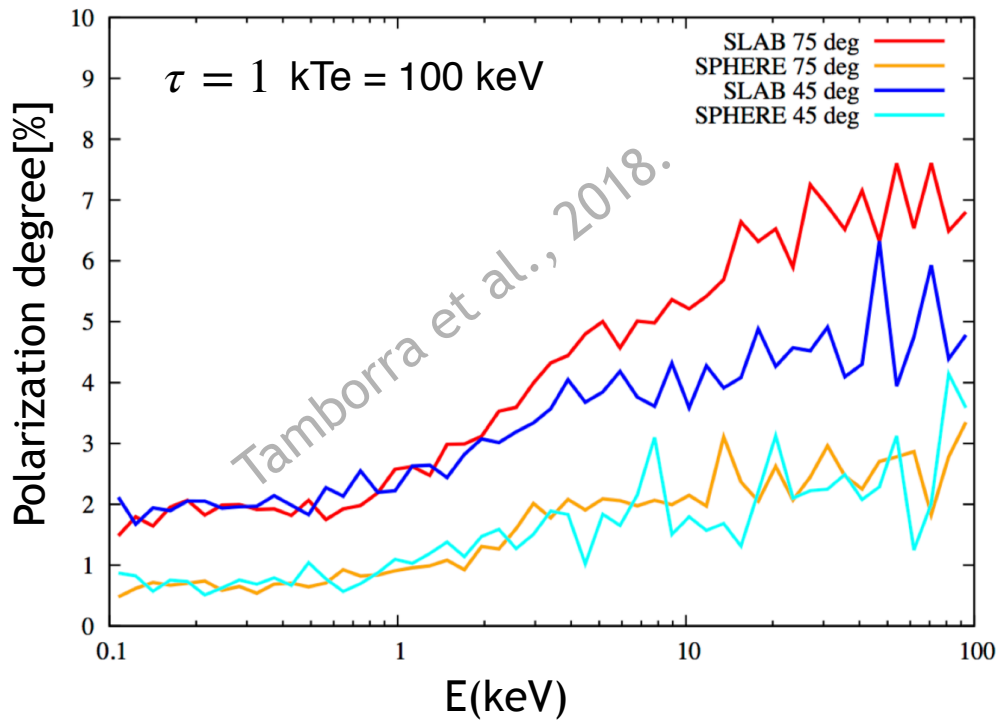
- Slab – high polarization (up to more than 10%): disc instabilities
- Sphere – very low polarization: aborted jet?



The AGN X-ray emission depends on the scattering processes in the corona. This dependency makes polarization studies a promising way to distinguish between different corona geometries.

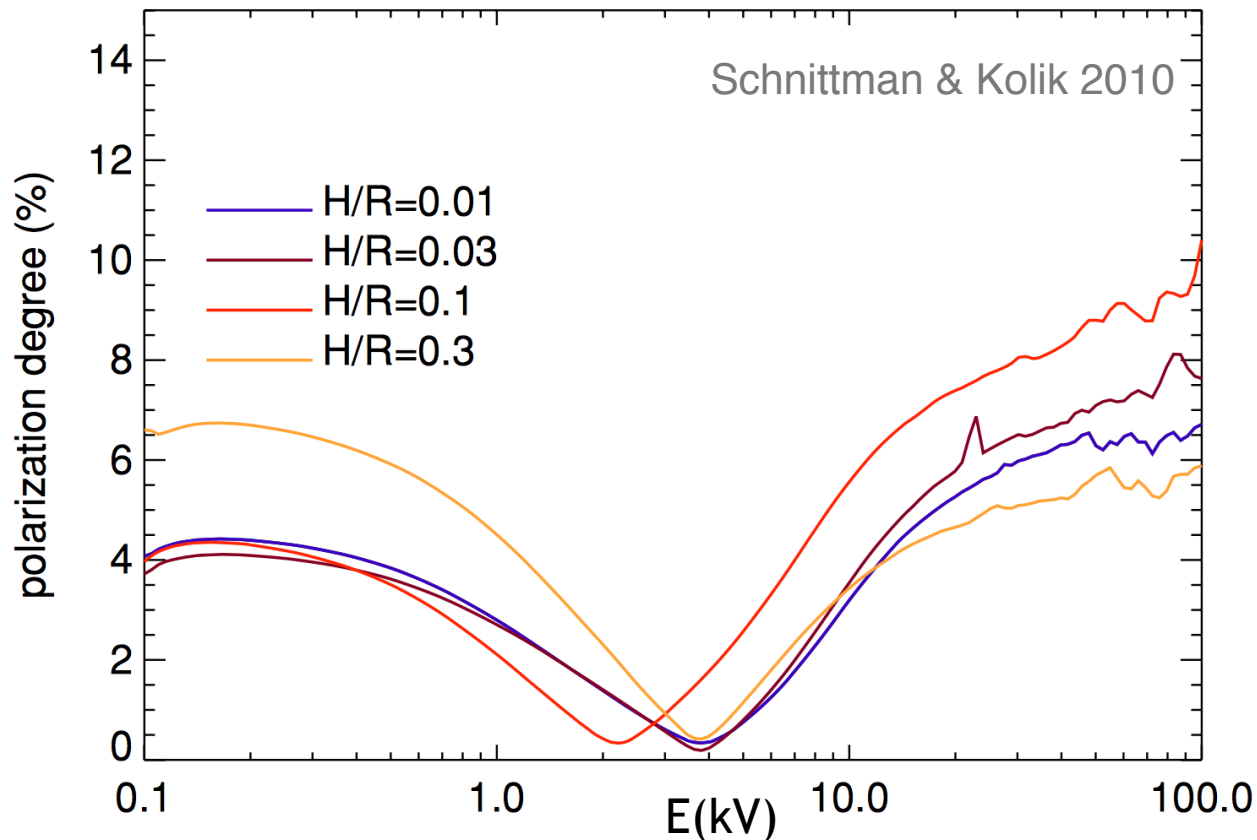
# HOT CORONAE AND POLARIZATION

Primary X-ray emission is expected to be polarized, the polarization degree depending mainly on the geometry and optical depth of the corona.



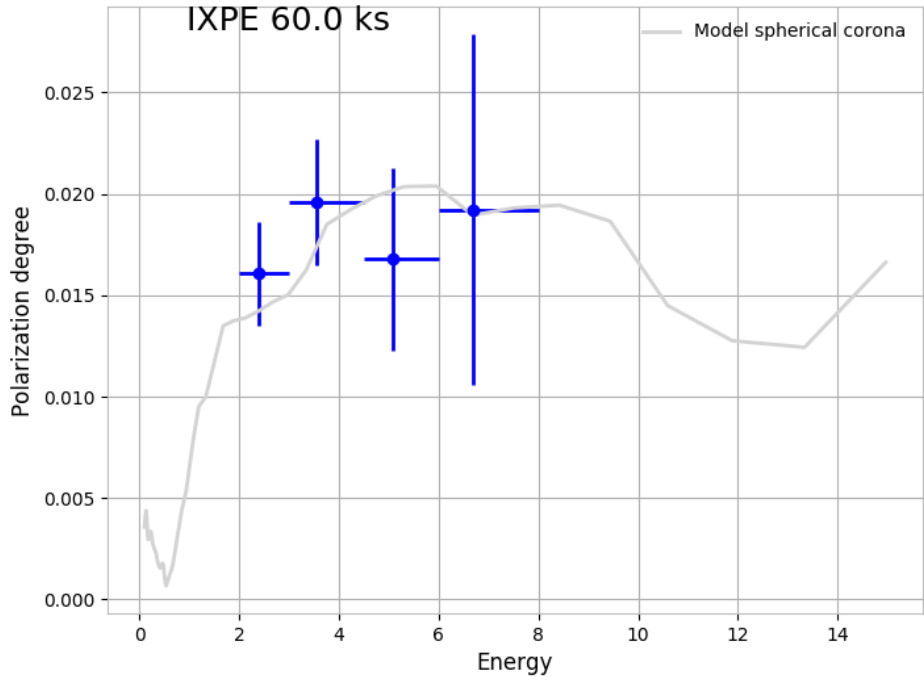
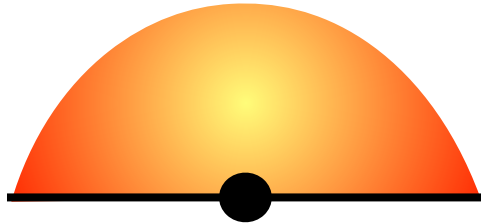
# HOT CORONAE AND POLARIZATION

Primary X-ray emission is expected to be polarized, the polarization degree depending mainly on the geometry and optical depth of the corona.

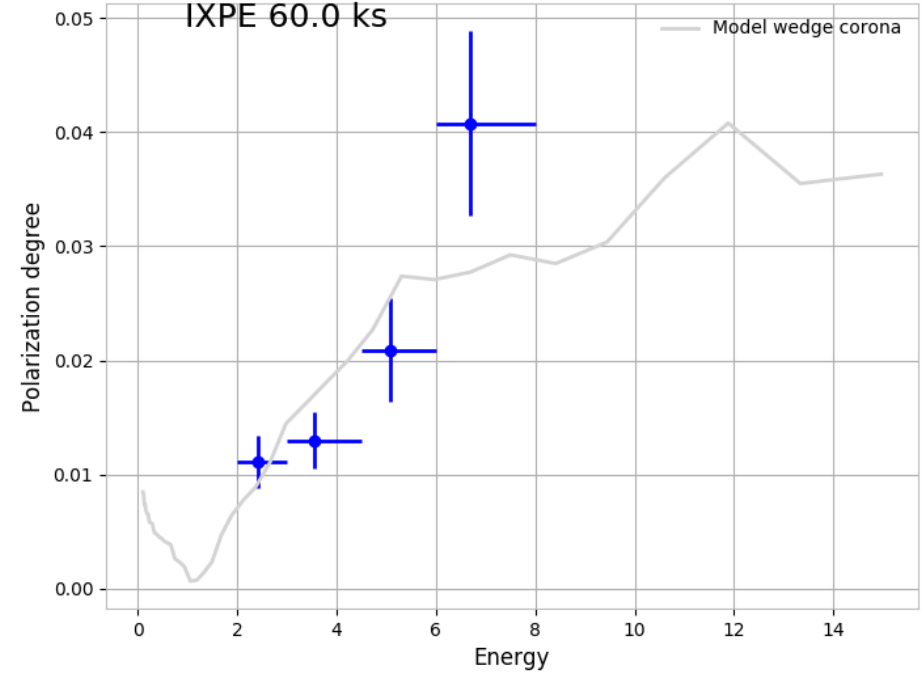


# CYGNUS X-1 SIMULATIONS

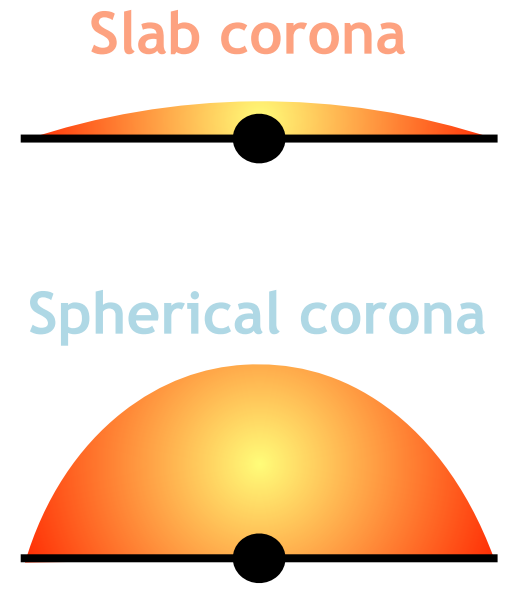
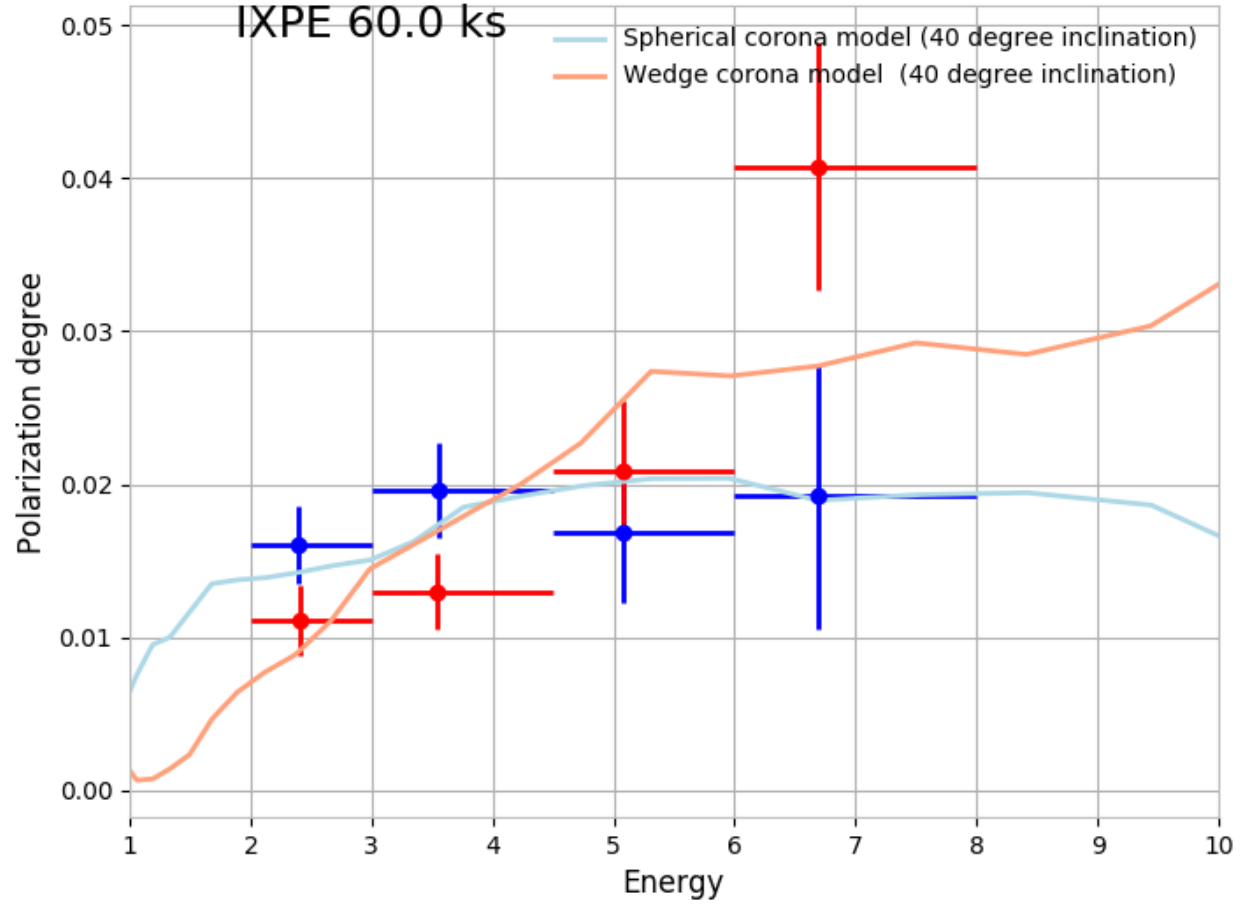
## Sphere



## Slab



# CYGNUS X-1 SIMULATIONS



- No correlation between  $E_c$  and  $\Gamma$ ;
- No large systematics in the *NuSTAR* measurements;
- Strong anti-correlation between the  $\tau$  and  $kT_e$  in slab or spherical geometries;
- Disk-corona in radiative equilibrium, but requires differences, from source to source, in either the coronal geometry or in the intrinsic disk emission;
- In none of the objects of the sample, X-ray spectroscopy has led to a clear discrimination between different coronal geometries.
- Waiting for IXPE for better results and discrimination about coronal geometry.

**THANK YOU!!!**

